

NaCl-dependent ordering and dynamic mechanical response in nanoconfined water

Shah H. Khan¹, Edward Kramkowski², Peter M. Hoffmann²

Abstract:

Understanding the dynamics of water under nanoscale confinement is important for biology, geology, tribology, and nanotechnology. In many naturally occurring situations, ions are present in water at various concentrations. Here, we report on how the addition of sodium ions alters the squeeze-out behavior of water nanoconfined between a mica surface and silicon oxide tip. We find that Na⁺ ions enhance molecular ordering and lead to longer mechanical relaxation times. We also observed a critical ion concentration above which the confined water switches from a viscous to an elastic (solid-like) response at very slow, quasistatic compression speeds.

Introduction

Nanoconfined water plays an important role in many situations related to biology, geology, tribology, colloid science and nanotechnology. Under nanoconfinement, water exhibits a number of unusual properties, including ordering, viscoelasticity and long relaxation times, although many details are still under discussion^{1, 2, 3, 4, 5, 6, 7, 8}. The presence of ions is expected to influence solid-water interfaces and confined water layers⁹. Ions change water properties due to their interactions with water's polar molecules, leading to solvation effects and changes in the hydrogen bonding structure. Initial work on the study of interaction between charged bodies in aqueous electrolyte solutions was carried out by Hofmeister who ranked salts according to their effects on protein precipitation¹⁰. Typically, Hofmeister effects are observed at medium to high salt concentrations of 10 – 1000 mM¹¹. Ions can be divided into chaotropes and kosmotropes depending on their effect on the hydrogen bonding network of water¹². Sodium ions, for instance, with their relatively small size and large charge density, are weak kosmotropes. They bind strongly to water and have large hydration enthalpy and negative hydration entropy.¹³

Some of the first direct measurements of forces between solid surfaces mediated by confined aqueous electrolytic solutions were performed by Israelachvili and Adam¹⁴, Israelachvili and Pashley,^{14, 15} and Pashley^{16, 17}. Israelachvili and Adam first saw clear deviations at small separations from the expected van-der-Waals and electrical double layer forces in a solution of KNO₃. Pashley¹⁷ studied LiCl, KCl, NaCl and CsCl electrolytes at various concentrations confined between mica sheets and found a critical concentration specific to each electrolyte above which strong repulsive hydration forces appeared below a separation of 2 nm. As in the measurements by Israelachvili and Adam, this could not be explained by double-layer forces, but instead was attributed to ionic hydration near the mica surfaces. The critical concentrations he observed ranged from 1 mM (KCl, CsCl) to 10 mM (NaCl) and 60 mM (LiCl) at pH~5.4. Repulsive forces could be removed by lowering the pH of the solution i.e. replacing the surface K⁺ with H⁺.¹⁶ Israelachvili and Pashley¹⁵ studied 1 mM KCl to further investigate the origin of hydration forces. Their studies revealed the presence of strongly oscillatory repulsive hydration forces at a separation of less than 1.5 nm. The oscillations showed small negative minima at film thicknesses of less than 1 nm.

More recent studies have shown a variety of effects of ions on structure, forces, and dynamics of nanoconfined water. For example, several studies investigated the influence of the chemistry of the confining surfaces^{18,19} as well as pH^{20, 21, 22} on the structure and mechanical response of the confined water. There are also questions about the effect of ions on the dynamics of water molecules. At fast timescales (pico- to nanoseconds), which cannot be accessed by AFM or SFA, ions play an important role in modifying the dynamics of water molecules, even well beyond the first hydration shell^{23, 24}. In our measurements, we probe much longer timescales, associated with the collaborative relaxation of large groups of molecules, leading to viscoelastic responses on time scales in the microsecond to second range^{3, 4, 25}. How the modifications of the water dynamics at fast timescales play into the observed long times-scale behavior is an important question that is difficult to answer, because current capabilities in computer simulations cannot access time scales above the nanosecond range, and there are few experimental approaches that can span time scales ranging from picoseconds to seconds. It is possible that as fast molecular relaxations of water molecules are affected by the presence of ions, they influence the average structure of water layers and have a strong effect on collective motions, which can be probed by SFA or AFM.

Computational studies of confinement experiments have also been performed. Studies by Leng²⁶, Argyris et al.²⁷ and He et al.²⁸ suggest that the presence of small monovalent ions enhances the stiffness of the layers due to the tight hydration shells²⁶. Regardless of the ion concentration, at neutral pH there are always ions adsorbed on mica to compensate the surface charge. However, when ions are added, there is an additional diffuse layer of ions 4-5 Å from the surface^{26, 29}. This layer becomes compressed upon confinement and is ultimately forced to adsorb. These dynamics lead to additional repulsive forces, as discussed in the early studies by Pashley and Israelachvili^{14, 16, 17}.

Here, we present measurements that probe two dynamic processes: the mechanical relaxation of water layers at various NaCl concentrations under dynamic load and the time scale of layer-by-layer squeeze-out under an approaching AFM tip. We investigate the effect of ion concentration on these dynamical processes, as well as on the structure of the nanoconfined electrolyte.

Experimental

Sodium chloride (>99% purity) was obtained from Fisher Scientific. Water was purified using a two-stage water purification system. In the first stage, water was purified using reverse osmosis to an ion concentration of less than 10 ppm. Then the water was further polished using a Siemens PURELAB classic UV/UF system. This system gave water at resistivity 18.2 MΩ-cm (ion concentration below detection levels) with low organic contamination levels. The pH of the water was not adjusted and measured to be close to 7. Water from the same source was also used for rinsing and cleaning the cantilever and the glass dishes. The Fisher brand micropipette was used to transfer water to the cell. The micropipette was soaked in concentrated HCL (11.6M) overnight before repeatedly rinsing with clean water. The glass dishes were kept overnight in saturated NaOH isopropanol solution and rinsed in ultrapure water.

A home-built small-amplitude AFM^{30, 31} was used to record changes in the amplitude and phase of the cantilever tip while the substrate slowly approaching towards the cantilever. An optical

fiber was aligned to the back of the cantilever to measure changes in the amplitude with a resolution better than 0.1 \AA using fiber interferometry. The cantilever was vibrated with amplitudes of less than 1 \AA at frequencies ranging from 400-1000 Hz, well below the 1st resonance frequency.

To perform an experiment, freshly cleaved mica was mounted in a clean liquid cell, made of a steel backing, a Kalrez O-ring and a Kel-F body. The cell was magnetically mounted on the AFM sample holder. About 1 ml of water was then transferred to the liquid cell using a clean micropipette. Using the auto-approach of the AFM, the cantilever was brought near to the mica surface while the cantilever was oscillated at small amplitude until a preset setpoint in amplitude was reached. At this point, the cantilever and fiber end were completely immersed in water. During the force measurement, the AFM feedback was suspended while the cantilever approached and retracted from the substrate. The change in amplitude and phase were measured with the help of a lock-in amplifier using the signal obtained from the fiber interferometer. Because of the very low approach speed, a single measurement could take several minutes. The reproducibility of low-noise measurements was between 20-30 % depending upon the mechanical and electrical noise of the surroundings, as well as drift during the measurement. Stiffness and damping were determined from the amplitude and phase by modeling the lever as a Kelvin-Voigt element in the small-amplitude, far-below-the-resonance case.^{3, 30, 32, 33}

Cantilevers were obtained from Nanosensors (PPP-FMR). Stiffnesses ranged from 1.4 N/m to 2 N/m. Cantilevers were cleaned in piranha solution for one hour at 80° C and then rinsed with deionized water from the above-stated system. This processing is necessary to remove organic contaminant and render the tip hydrophilic. The cantilever stiffness was calibrated using both the geometrical method and the thermal method³⁴. Effective tip sizes were quite large (ranging from a few 100 nm to over 1 \mu m), therefore allowing us to measure the collective dynamics of nanoconfined mesoscopic water layers. The reason for the large tip sizes is that the long lock-in integration times we had to use are not effective in maintaining feedback during approach of the tip to the surface. As a result, the tip becomes dulled and templated against the flat mica substrate. This dulling process enhances the signal and allows us to study squeeze-out processes. A typical tip structure used in our experiments is shown in Figure 1.

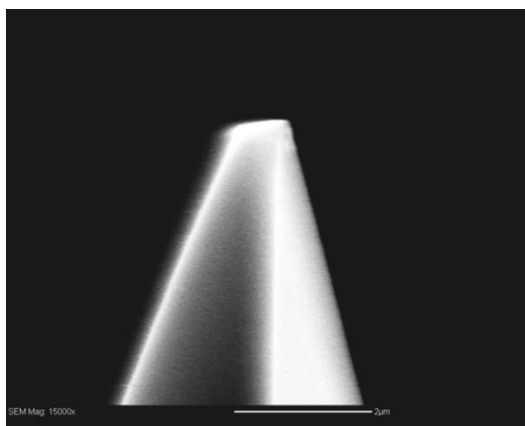


Figure 1: SEM image of typical tip used in experiment, blunted and flattened to a radius of about 1 \mu m .

To minimize the effect of external vibrations, the AFM was placed on a vibration isolation platform (Minus K BM4). To keep the AFM from sound waves, a double box setup was used. The inside box holds the Minus K system and the AFM. Its walls were made of steel (outside) and thick foam sheets (inside). This small box was then included in a telephone-booth-sized box. This box was made of high density hard board of thickness 2.5 cm to effectively block the outside noise. Further vibration isolation was provided by using vibration isolation rubber pads in two stages. A series of rubber pads in the first stage separates the large soundproof box, about 1.8 m high and 1 m wide, from the ground. The second series of rubber pads separates the smaller box from the outer sound box to reduce vibrations.

Results and Discussion

Figure 2 shows representative plots of the measured stiffness, damping and Maxwell relaxation time³⁵ at three different NaCl concentrations – 0 (de-ionized water), 1 and 1000 mM NaCl. The compression rate at which these measurements were performed was 2 Å/s. The Maxwell relaxation time t_R was calculated according to $t_R = \frac{k}{\omega^2 \gamma}$,³ where k is the stiffness, γ is the damping coefficient, and ω is the frequency of oscillation of the cantilever.

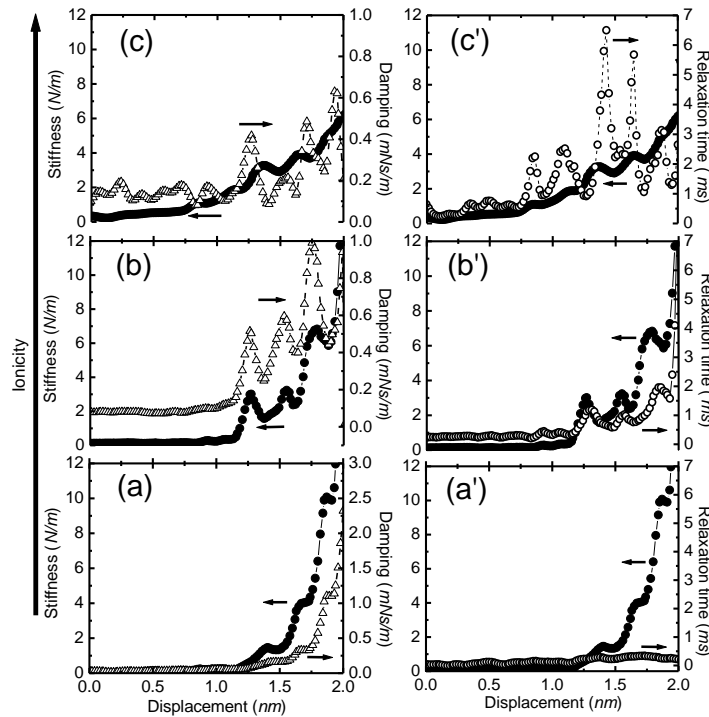


Figure 2: Stiffness, damping and Maxwell relaxation times for pure water (a, a'), 1 mM NaCl (b, b') and 1 M NaCl (c, c') at a compression rate of 2Å/s. Adding NaCl ions enhances ordering and leads to an increasing elastic response upon ordering, evidenced by the peaks in the Maxwell relaxation times.

In all cases, the stiffness of the layers follows a monotonic increase, with stiffness oscillations superimposed upon it. The monotonic increase is due to hydration repulsion, as is typically seen in pure water or water containing small ions^{4, 17, 36}. Pashley found hydration only above a critical concentration. However, the majority of more recent results have shown repulsive hydration forces even at very small ion concentration¹⁵ or in pure water^{1, 3, 6, 9, 15, 37, 38}.

The observed stiffness oscillations have an average period of $2.6 \pm 0.8 \text{ \AA}$, commensurate to the molecular size of water³⁹. This period was determined from a total of about 260 successful measurements. The number of peaks associated with molecular ordering increases from three to five as the ion concentration is increased, as was also observed by Kilpatrick et al⁹. This suggests that adding NaCl enhances liquid ordering, consistent with the fact that sodium is considered a mild kosmotrope, i.e. an order enhancer in water. In the case of pure water, the stiffness oscillates *in-phase* with the damping coefficient atop a monotonically increasing background as the sample and the cantilever get closer (Figure 2a). This type of relationship between stiffness and damping coefficient gives rise to a constant profile in the relaxation time (Figure 2 a'), with an average bulk value of $\tau_{RB} = 5 \times 10^{-4} \text{ s}$. At 1mM NaCl (Figure 2b, b'), the stiffness and damping also oscillate in unison as a function of distance, giving rise to a nearly uniform profile of the relaxation time (Figure 2b' circles). However, small peaks can be seen in the relaxation time towards the right (when the film thickness equals two layers) which indicate subtle changes in the dynamics of the film.

The situation is significantly different at 1M NaCl (Figure 2c, c'). The damping coefficient in these measurements is *out-of-phase* with the stiffness as the sample approaches the cantilever. This behavior introduces orders of magnitude increases in the relaxation time (Figure 2c' circles) as compared with the bulk. In most cases, peaks in the relaxation time are associated with oscillations in the stiffness and damping that are out-of-phase with each other. In rare cases, we observed relaxation time peaks when the stiffness and damping were in-phase, but the stiffness increased much faster than damping³⁵. These differences could be due to small changes in local tip structure, but this is difficult to ascertain. However, for all tips we found clearly distinguishable differences between measurements with in-phase versus out-of-phase damping. These observations only depended on ion concentration and approach speed, not on the particular tip geometry.

The increase in the relaxation time associated with a stiffness peak and a decrease in damping is referred to as dynamic solidification⁴, because it indicates a sharp increase in the elastic response and a corresponding decrease in the viscous response of the water layer. This crossover in behavior occurs at a characteristic time scale of a few 100 ms, which is much slower than single molecular relaxation times. This points to a cooperative mode of motion as the liquid is compressed between the two surfaces. Thus the observed solidification is a viscoelastic phenomenon, involving many molecules moving collaboratively during squeeze-out.

Our observations suggest that higher salt concentration (1M NaCl) causes the water layers to behave more elastically in comparison with pure water or low salt concentration (1mM NaCl). In our previous work on pure water, elastic behavior was only visible at an approach speed of at least 8 \AA/s , which we suggested as critical speed for dynamic solidification⁴. In Figure 2, the comparison of pure water and a 1 M NaCl solution shows that dynamic solidification is observed at as small an approach speed as 2 \AA/s if a high enough concentration of NaCl is present.

While the range of ordering and the onset of dynamic solidification showed a clear dependence on the ion concentration, the magnitudes of stiffness and damping were primarily determined by the details of the tip shape⁴⁰. Because of varying tip shapes, we were not able to ascertain a general dependence of the stiffness and damping magnitudes on the ion concentrations, even when trying to account for the effective tip radii.

As in our previous work^{4, 35}, we looked at the behavior of the confined water films at various dynamic compression rates. We took measurements over a range of approach speeds, from 4 to 16 Å/s.

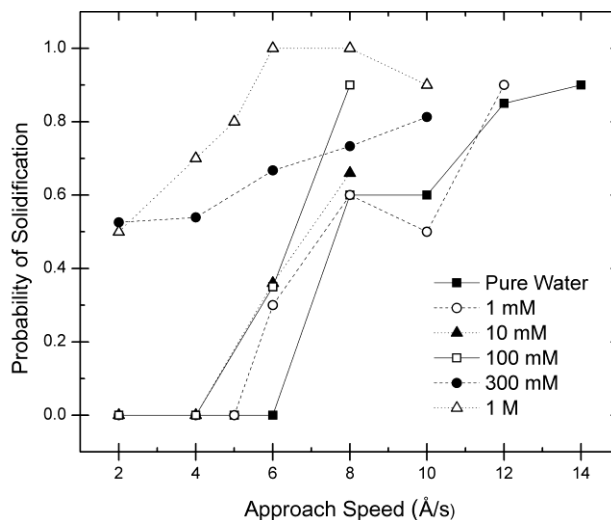


Figure 3: Fraction of measurements that showed an elastic (solid-like) response versus compression rate for different NaCl concentration. It can be seen that at low concentrations of NaCl, the response of the confined water layers changes slowly, but between 100 and 300 mM, there is a pronounced change in response.

Figure 3 summarizes our findings. It shows the fraction of measurements that showed an elastic (solid-like) response to compression, i.e. the probability of dynamic solidification, as a function of compression rate for various Na⁺ concentrations. Here we see that the addition of Na⁺ ions not only enhances order, but also increases the propensity for the layers to become “jammed”⁴ leading to an elastic response at lower compression speed. This suggests a significant increase in relevant relaxation times as ion concentration increases, associated with a restructuring of the layers as they are compressed and squeezed out^{41, 42}. A significant change in this behavior is observed between ion concentrations of 100 – 300 mM. Below this range, the difference in behavior between pure water and water with some NaCl is rather small. Therefore, there seems to be a critical sodium concentration between 100- 300 mM, at which an elastic response under slow compression become significantly more prevalent.

This is better seen in Figure 4, where we plotted the speed at which there is at least a 50% chance of an elastic response (threshold speed) versus NaCl concentration. The dependence of the threshold speed versus concentration is sigmoidal, similar to a titration curve. It clearly shows the crossover at a critical concentration of about 200 mM. The reason for this behavior is not known. As discussed by Leng²⁶, there are always sufficient ions present to compensate for the negative surface charge of mica at neutral pH. Any additional ions locate in a diffuse layer

and are forced to adsorb when the liquid is compressed. It is possible that below about 200 mM, additional ions can be relatively easily accommodated, but above this critical concentration, repulsion between excess ions and the resulting rearrangement of the adsorbed layer leads to slow dynamics.

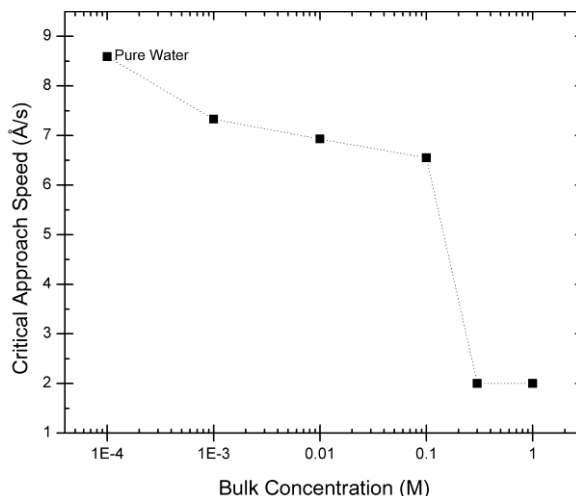


Figure 4: Approach speed at which 50% of measurements show an elastic (solid-like) response versus NaCl concentration. The pure water data point is included for reference only.

As mentioned above, Pashley¹⁷ observed critical concentrations at which repulsive hydration forces greatly increased. The concentrations Pashley observed for the increased hydration forces were lower (10 mM for NaCl) than the critical concentration we observed at which we see a clear change in dynamic behavior. Nevertheless, the origin of the two transitions may be similar: Pashley suggested that at some sufficiently high concentration, it becomes energetically favorable for ions to remain on the surface rather than be exchanged for H^+ ions as the liquid layer is compressed. This is consistent with the simulations by Leng²⁶. The differences in the critical concentration may be due to the differences in confining surfaces –mica/mica in the case of Pashley’s experiments, and mica/silicon oxide in our experiments⁴³.

An important point to make here is that with increasing Na^+ concentration, we also increase the concentration of Cl^- . Because of the negative charge of chlorine ions, they do not adsorb close the negatively charged mica surface and therefore do not form the tight hydration layers formed by the cation^{44, 45}. As has been found in simulations, the cations form strong “load bearing”, adsorbed hydration shells²⁶. Moreover, Cl^- has been found to have faster diffusion and is not incorporated into a “dynamically hindered hydration layer” near the surface²⁷. Since our measurements probe the highly slowed down dynamics of confined hydration layers, the agile and weakly bound anions are not expected to play a major role in the here presented observations. Nevertheless, future studies should explore the effect of changing the anion species.

Figure 5 shows the peak Maxwell relaxation times for one to five molecular layers of water and four representative ion concentrations, including 300 mM, at 0.2 nm/s approach speed.

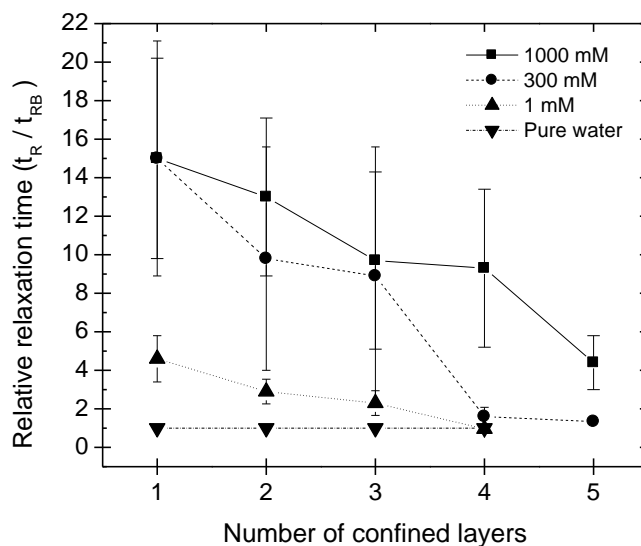


Figure 5: Peak mechanical relaxation times (ratio of peak relaxation time to bulk relaxation time) versus the number of confined layers in water for 1 M (squares/Solid line), 300 mM (circles, dashed line), 1 mM NaCl (up triangles/dotted line), and pure water (down triangles/dotted line). The squeeze rate was 0.2 nm/s in all the cases.

Peaks in the Maxwell relaxation time indicate elastic behavior. Elastic effects are not observed in pure water at such a low compression speed, but weak effects are seen in the 1 mM case ≤ 0.75 nm from the surface. Adding further ions, to above 100 mM, increases the thickness of water films exhibiting an elastic response at 0.2 nm/s compression speed to above 1 nm (up to five molecular layers). At these high ion concentrations, relaxation times are significantly increased, corresponding to a more pronounced elastic response. For example, for a single molecule thick film, the addition of 1 M NaCl increases the relaxation time by a factor of three over the value for 1 mM of NaCl.

Summary and Conclusions

We have shown that the addition of ions has a profound effect on the squeeze-out dynamics of nanoconfined water. Na^+ ions enhance ordering and lead to longer mechanical relaxation times. Moreover, we observed a critical concentration at which the dynamics changes dramatically, from a liquid-like response to a solid-like (elastic) response under essentially quasi-static compression speeds (2-4 Å/s). These observations are consistent with the notion that at sufficiently high ion concentrations, hydrated ions adsorb on the mica surface and become difficult to replace as the liquid is compressed.

Acknowledgements

P.M.H. would like to acknowledge funding through the National Science Foundation grant DMR 0804283, and through Wayne State University.

References

1. Antognozzi, M.; Humphris, A. D. L.; Miles, M. J. Observation of molecular layering in a confined water film and study of the layers viscoelastic properties. *Appl Phys Lett* **2001**, *78* (3), 300-302.
2. Cleveland, J. P.; Sch; auml; ffer, T. E.; Hansma, P. K. Probing oscillatory hydration potentials using thermal-mechanical noise in an atomic-force microscope. *Physical Review B* **1995**, *52* (12), R8692.
3. Jeffery, S.; Hoffmann, P. M.; Pethica, J. B.; Ramanujan, C.; Özer, H. Ö.; Oral, A. Direct measurement of molecular stiffness and damping in confined water layers. *Physical Review B* **2004**, *70* (5), 054114.
4. Khan, S. H.; Matei, G.; Patil, S.; Hoffmann, P. M. Dynamic Solidification in Nanoconfined Water Films. *Phys Rev Lett* **2010**, *105* (10), 106101.
5. Lim, L. T. W.; Wee, A. T. S.; O'Shea, S. J. Effect of Tip Size on Force Measurement in Atomic Force Microscopy. *Langmuir* **2008**, *24* (6), 2271-2273.
6. Raviv, U.; Laurat, P.; Klein, J. Fluidity of water confined to subnanometre films. *Nature* **2001**, *413* (6851), 51-54.
7. Zhu, Y.; Granick, S. Viscosity of Interfacial Water. *Phys Rev Lett* **2001**, *87* (9), 096104.
8. Fukuma, T.; Ueda, Y.; Yoshioka, S.; Asakawa, H. Atomic-Scale Distribution of Water Molecules at the Mica-Water Interface Visualized by Three-Dimensional Scanning Force Microscopy. *Phys Rev Lett* **2010**, *104* (1), 016101.
9. Kilpatrick, J. I.; Loh, S. H.; Jarvis, S. P. Directly Probing the Effects of Ions on Hydration Forces at Interfaces. *Journal of the American Chemical Society* **2013**, *135* (7), 2628-2634.
10. Hofmeister, F. Zur Lehre von der Wirkung der Salze. [About the science of the effect of salts.]. *Arch Exp Pathol Pharmacol* **1888**, *24*, 247-260.
11. Cacace, M. G.; Landau, E. M.; Ramsden, J. J. The Hofmeister series: salt and solvent effects on interfacial phenomena. *Quarterly Reviews of Biophysics* **1997**, *30* (3), 241-277.
12. Frank, H. S.; Wen, W. Y. Structural Aspects of Ion-Solvent Interaction in Aqueous Solutions - a Suggested Picture of Water Structure. *Discussions of the Faraday Society* **1957**, (24), 133-140.
13. Collins, K. D. Charge density-dependent strength of hydration and biological structure. *Biophys J* **1997**, *72* (1), 65-76.
14. Israelachvili, J. N.; Adams, G. E. Measurement of forces between 2 mica surfaces in aqueous-electrolyte solutions in range 0-100 nm. *Journal of the Chemical Society-Faraday Transactions I* **1978**, *74*, 975.
15. Israelachvili, J. N.; Pashley, R. M. Molecular layering of water at surfaces and origin of repulsive hydration forces. *Nature* **1983**, *306* (5940), 249-250.
16. Pashley, R. M. Hydration forces between mica surfaces in aqueous electrolyte solutions. *J Colloid Interf Sci* **1981**, *80* (1), 153-162.
17. Pashley, R. M. DLVO and hydration forces between mica surfaces in Li⁺, Na⁺, K⁺, and Cs⁺ electrolyte solutions: A correlation of double-layer and hydration forces with surface cation exchange properties. *J Colloid Interf Sci* **1981**, *83* (2), 531-546.

18. Chapel, J. P. Electrolyte Species Dependent Hydration Forces between Silica Surfaces. *Langmuir* **1994**, *10* (11), 4237-4243.
19. Vakarelski, I. U.; Ishimura, K.; Higashitani, K. Adhesion between Silica Particle and Mica Surfaces in Water and Electrolyte Solutions. *J Colloid Interf Sci* **2000**, *227* (1), 111-118.
20. Boström, M.; Deniz, V.; Franks, G. V.; Ninham, B. W. Extended DLVO theory: Electrostatic and non-electrostatic forces in oxide suspensions. *Advances in Colloid and Interface Science* **2006**, *123–126* (0), 5-15.
21. Dishon, M.; Zohar, O.; Sivan, U. From Repulsion to Attraction and Back to Repulsion: The Effect of NaCl, KCl, and CsCl on the Force between Silica Surfaces in Aqueous Solution. *Langmuir* **2009**, *25* (5), 2831-2836.
22. Ulcinas, A.; Valdre, G.; Snitka, V.; Miles, M. J.; Claesson, P. M.; Antognozzi, M. Shear Response of Nanoconfined Water on Muscovite Mica: Role of Cations. *Langmuir* **2011**, *27* (17), 10351-10355.
23. Park, S.; Moilanen, D. E.; Fayer, M. D. Water Dynamics The Effects of Ions and Nanoconfinement. *The Journal of Physical Chemistry B* **2008**, *112* (17), 5279-5290.
24. Hewish, N. A.; Enderby, J. E.; Howells, W. S. The Dynamics of Water-Molecules in Ionic Solution. *J Phys C Solid State* **1983**, *16* (10), 1777-1791.
25. Patil, S.; Matei, G.; Oral, A.; Hoffmann, P. M. Solid or liquid? Solidification of a nanoconfined liquid under nonequilibrium conditions. *Langmuir* **2006**, *22* (15), 6485-6488.
26. Leng, Y. S. Hydration Force between Mica Surfaces in Aqueous KCl Electrolyte Solution. *Langmuir* **2012**, *28* (12), 5339-5349.
27. Argyris, D.; Cole, D. R.; Striolo, A. Ion-Specific Effects under Confinement: The Role of Interfacial Water. *Acs Nano* **2010**, *4* (4), 2035-2042.
28. He, Y.; Shao, Q.; Chen, S. F.; Jiang, S. Y. Water Mobility: A Bridge between the Hofmeister Series of Ions and the Friction of Zwitterionic Surfaces in Aqueous Environments. *J Phys Chem C* **2011**, *115* (31), 15525-15531.
29. Sakuma, H.; Kawamura, K. Structure and dynamics of water on muscovite mica surfaces. *Geochimica Et Cosmochimica Acta* **2009**, *73* (14), 4100-4110.
30. Patil, S.; Matei, G.; Dong, H.; Hoffmann, P. M.; Karakose, M.; Oral, A. A highly sensitive atomic force microscope for linear measurements of molecular forces in liquids. *Review of Scientific Instruments* **2005**, *76* (10), 103705.
31. Patil, S. V.; Hoffmann, P. M. Small-amplitude atomic force microscopy. *Adv Eng Mater* **2005**, *7* (8), 707-712.
32. Hoffmann, P. M. Small-Amplitude Atomic Force Microscopy. In *Dekker Encyclopedia of Nanoscience and Nanotechnology*; CRC Press, 2004.
33. Patil, S. V.; Hoffmann, P. M. Small-Amplitude Atomic Force Microscopy. *Advanced Engineering Materials* **2005**, *7* (8), 707-712.
34. Matei, G. A.; Thoreson, E. J.; Pratt, J. R.; Newell, D. B.; Burnham, N. A. Precision and accuracy of thermal calibration of atomic force microscopy cantilevers. *Review of Scientific Instruments* **2006**, *77* (8), 083703-6.
35. Khan, S. H.; Hoffmann, P. M. Squeeze-out dynamics of nanoconfined water: A detailed nanomechanical study. *Physical Review E* **2015**, *92* (4).
36. Perkin, S.; Goldberg, R.; Chai, L.; Kampf, N.; Klein, J. Dynamic properties of confined hydration layers. *Faraday Discuss* **2009**, *141*, 399-413.
37. Li, T. D.; Gao, J. P.; Szoszkiewicz, R.; Landman, U.; Riedo, E. Structured and viscous water in subnanometer gaps. *Physical Review B* **2007**, *75* (11), 115415.

38. Sakuma, H.; Otsuki, K.; Kurihara, K. Viscosity and lubricity of aqueous NaCl solution confined between mica surfaces studied by shear resonance measurement. *Phys Rev Lett* **2006**, 96 (4).
39. Cheng, L.; Fenter, P.; Nagy, K. L.; Schlegel, M. L.; Sturchio, N. C. Molecular-scale density oscillations in water adjacent to a mica surface. *Phys Rev Lett* **2001**, 87 (15).
40. Khan, S. H.; Kramkowski, E. L.; Ochs, P. J.; Wilson, D. M.; Hoffmann, P. M. Viscosity of a nanoconfined liquid during compression. *Appl Phys Lett* **2014**, 104 (2).
41. de Beer, S.; den Otter, W. K.; van den Ende, D.; Briels, W. J.; Mugele, F. Non-monotonic variation of viscous dissipation in confined liquid films: A reconciliation. *Europhys Lett* **2012**, 97 (4).
42. Gosvami, N. N.; O'Shea, S. J. Nanoscale Trapping and Squeeze-Out of Confined Alkane Monolayers. *Langmuir* **2015**, 31 (47), 12960-12967.
43. Butt, H. J. Measuring Electrostatic, Vanderwaals, and Hydration Forces in Electrolyte-Solutions with an Atomic Force Microscope. *Biophys J* **1991**, 60 (6), 1438-1444.
44. Tournassat, C.; Chapron, Y.; Leroy, P.; Bizi, M.; Boulahya, F. Comparison of molecular dynamics simulations with triple layer and modified Gouy-Chapman models in a 0.1 M NaCl-montmorillonite system. *J Colloid Interf Sci* **2009**, 339 (2), 533-541.
45. Dequidt, A.; Devemy, J.; Malfreyt, P. Confined KCl Solution between Two Mica Surfaces: Equilibrium and Frictional Properties. *J Phys Chem C* **2015**, 119 (38), 22080-22085.

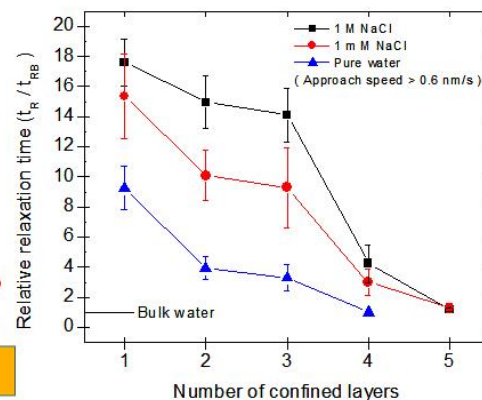
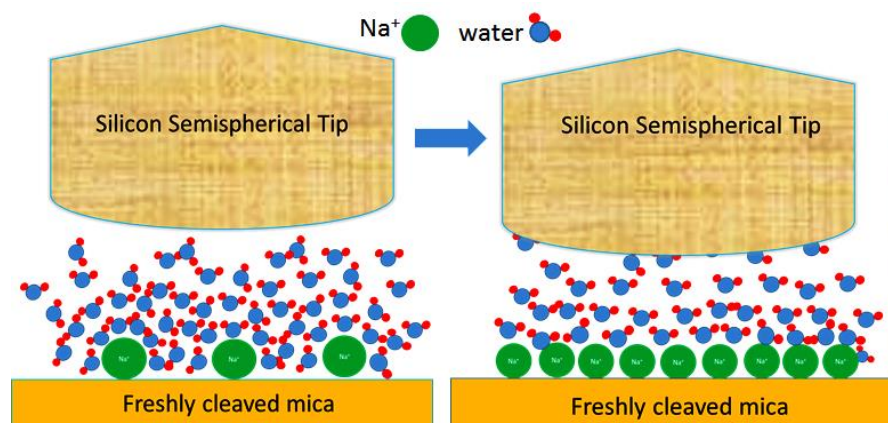


Figure for the Table of Contents